Quantum-based Gated Recurrent Units for Multiclass Classification to Monitor Daily Living Activities for Early Disease Detection

Bao-Nhi Dang Tran*, Muhammad Fahim†, Bradley D. E. McNiven*, Stephen Czarnuch*, Octavia A. Dobre*, and Trung Q. Duong*

*Memorial University, Canada (e-mail: {ntrandangbao, b.mcniven, sczarnuch, odobre, tduong}@mun.ca)
†Queen's University Belfast, United Kingdom (e-mail: {m.fahim, trung.q.duong}@qub.ac.uk)

***Abstract*—The continuous monitoring of activities of daily living (ADLs) can play a vital role in assessing an individuals capability to live independently and enable the possibility for early disease detection. This paper introduces a novel hybrid model, called quantum-based gated recurrent unit - multiclass classifier (QGRU-MC), to enhance ADL classification from wearable sensor data. Using statistical feature extraction from the raw accelerometer sensor signals, the QGRU-MC model demonstrates good performance in activity recognition. Preliminary findings suggest that our model has good potential in healthcare applications, and in particular, can contribute to the advancement of future intelligent systems centered on daily activity monitoring and the promotion of healthy aging.**

I. Introduction

The continuous and automatic monitoring of activities of daily living (ADLs) plays a critical role in ambient intelligence, especially within the field of gerontology for assessing an individual's capability for independent living [1]. Furthermore, monitoring ADLs allows for the early detection of potential health concerns such as Alzheimer's disease [2] and dementia [3]. Previous work has utilized sensing devices in experiments for ADLs classification [4]. In particular, wearable sensors, such as devices worn by humans on wrists, chest, or hips, are the preferred method for their low cost and high sensitivity and data granularity [5].

Among wearables sensor methods, tri-axial accelerometers are the reasonable choice for action, movement, and activity recognition due to their temporal dependencies between data points [1], [6], [7]. To effectively capture these dependencies, previous work has highlighted a set of signal processing and machine learning methods for ADL classification [4]. In particular, recurrent neural networks (RNNs), a sub-type of artificial neural networks that are commonly used in natural language processing [8] and speech recognition [9], have been used for activity recognition with the use of raw tri-axial accelerometer data and gyroscope for ADL classification [10].

With recent advancements in quantum hardware and algorithms, quantum machine learning (QML) techniques have emerged. Offering the potential to solve complex problems beyond the capabilities of classical machine learning, QML utilizes properties of quantum systems like entanglement and superposition and has since attracted attention from the research community as a method to process complex data. Specific promise has been shown in healthcare applications, such as the utility of electroencephalogram (EEG) abnormality prediction, and prediction of physical activity energy expenditure [11]–[13].

Within QML, variational quantum circuits (VQCs) [14] are commonly employed due to their ability to be iteratively optimized using optimization algorithms and demonstration of overall applicability regarding expressive power. These circuits have gained popularity because of their robustness against quantum noise, particularly in ever-growing noisy intermediate-scale quantum technology (NISQ) [15]. Additionally, there is an increasing amount of research demonstrating the stronger expressive power of VQCs compared to that of classical neural networks. Examples include the application of multi-parameterized quantum circuits for simulating probability distributions [16] and the use of quantum annealing techniques coupled with entanglement methods to address challenging classical problems [17].

In this paper, we propose a novel hybrid quantum-based algorithm gated recurrent unit (QGRU) that utilizes VQCs and is combined with a classical multiclass classifier. Referred to in this work as QGRU-MC, we aim to use it to classify ADL data collected from tri-axial accelerometers to improve upon the precision of frailty assessment and activity recognition for early detection of diseases. Based on preliminary results, QGRU-MC demonstrated a good performance in the prediction accuracy for tri-axial accelerometer time-series data and indicated it is robust in the handling of data from complex human movement patterns.

II. Dataset and data pre-processing

For the experiment and evaluation, we use the publicly available "Dataset for ADL Recognition with Wrist-worn Accelerometer" [18]. The data consists of tri-axial accelerometer recordings collected from a right wrist-worn device as participants performed 14 daily activities such as brushing teeth, climbing stairs, eating, and drinking. The raw sampling rate

was 32 Hz and was annotated. A sample of the acceleration for walking is presented in Fig 1.

During our analysis of the data, we re-label activities by grouping them into 8 different categories labeled 0 through 7. These mapping details are displayed in Table I.

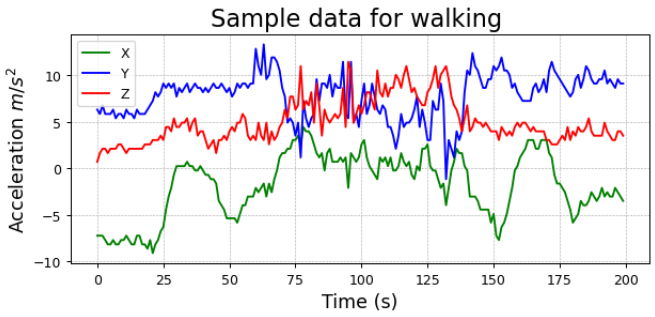

Fig. 1: Raw tri-axial accelerometer signal along the x-, y-, and z-axis from walking.

A. Pre-processing imbalance data

The class label distribution is heavily imbalanced when there are several classes with more data than others (see Table I). For example, the activity labeled "Telephone" (activity number 4) is only approximately 10% of the activity labeled "Eat and drink"(activity number 2) , which is 157 compared to 1272.

TABLE I: Activity labels and groupings.

Activity	Label	Values
Get up & lay down	0	593
Walk	1	959
Eat & drink	2	1271
Stairs	3	577
Telephone	4	157
Sit down & stand up	5	522
Brush teeth	6	309
Comb hair	7	243

To address the issue of imbalanced data, the synthetic minority over-sampling technique combined with edited nearest-neighbors (SMOTE-ENN) was employed. SMOTE is a resampling technique that synthesizes new instances for the minority class by interpolating between existing minority [19]. ENN is a data cleaning method that removes instances from both the majority and minority classes if their class labels do not match the majority of their nearest neighbors [20]. The dual strategy provides a more balanced and cleaner dataset, thereby improving the performance and robustness of the subsequent classification model. This in turn leads to a more reliable and generalized predictive model.

B. Feature Extraction

In order to effectively capture all essential characteristics of the acceleration data while maintaining a manageable computational requirement, we derive a compact set of features from the acceleration signal by calculating the statistical representation of the original data. Specifically, we divided the signal into 3-minute segments and then calculated the mean, median, standard deviation, interquartile range, and correlation among the three axes over each of these fixed-length windows, without any overlap between adjacent windows. This extracted feature method includes the computation of the above-mentioned statistical metrics and is proven to yield better activity classification, at least in dynamic activities studied in the healthcare domain [21]. For our case, these features are sufficient enough to offer good context-based information for the QGRU model.

III. Model Architecture

A. Variational Quantum Circuit block

Generally, the implementation of a VQC block consists of three main layers: the embedding layer, the variational layer, and the measuring layer.

1) Encoding Layer: Allows for the encoding of classical data into a quantum representation through the use of feature mapping. These features play a vital role in converting classical input data into a set of gate parameters that generate the corresponding quantum state. In this work, our encoding layer consists of amplitude encoding, which encodes data as amplitudes of the quantum state. This facilitates efficient data manipulation and processing within the quantum algorithm.

2) Variational Layer: At the heart of the VQC, the variational layer controls the entanglement and rotation of a circuit qubit to facilitate complex, non-linear mapping of information [22]. The efficacy of these mappings has a significant impact on the prediction accuracy of QML models. For our QGRU-MC model, we utilize enhanced controlled-Z rotation (CRZ) for quantum entanglement and for circuit block connectivity patterns. The implementation of the proposed model can improve the circuit's learning ability in two key ways.

Firstly, the CRZ implementation rotates qubits along the Z-axis, allowing variational rotation to occur during the quantum entanglement process. Consequently, this allows qubits to utilize quantum entanglement for rotations.

Secondly, the circuit block configuration arranges the qubit in a natural way that forms a closed loop. This pattern incorporates both local and non-local connections and facilitates a balance between simplicity and connectivity. Each circuit block in this structure is designated to employ qubits organized in a manner that forms a cyclic loop, as illustrated in Fig 2. This allows the interaction between consecutive and non-consecutive qubits. This approach has been shown to be advantageous for near-term quantum devices in terms of optimization of expressibility and entangling power of the quantum circuit [23].

Finally, after a series of CRZ gates, there are three rotation angles that correspond to each of the three axes ($R_n = R(\theta_n\omega_n, \phi_n)$) in the single-qubit rotation gates that are also adjusted iteratively during the optimization process by method of gradient descent.

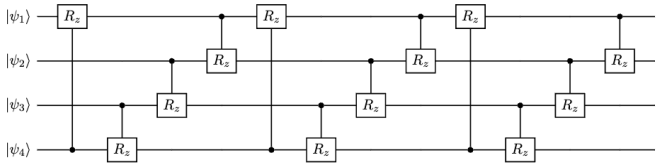

Fig. 2: Variational Quantum Circuit (VQC) implementation utilizing CRZ gates for qubit rotations along the Z-axis during quantum entanglement.

3) Measurement Layer: After the computational process of each VQC, there is a measurement layer. In the proposed model, this involves measuring the probabilities of computational basis states in the basis of the Pauli-Z operator. On classical computers, the calculation is performed numerically using quantum simulator software that offers zero-noise quantum computation. The measurement process generates a fixed-length vector that is subsequently processed by the classical computer for making predictions.

B. Quantum Gated Recurrent Unit

Our QGRU-MC model is an extension of classical GRU by integrating quantum-based algorithms into its architecture. The key idea is the replacement of classical neural network components with VQCs in all GRU gates that can properly utilize the computational advantages offered by quantum computation. Similar to the classical case, QGRU also contains cells that act as both memory and gates which modify the flow of information to the next layers. The QGRU contains two gates which are reset and updated. The reset gates decide which information must be removed from the memory cell, while the update gate determines which information should be refreshed. These manipulations allow the model to retain long sequences of information without losing important relevant details. An implementation of the QGRU with support of a linear embedding layer model is shown in Fig 3 to illustrate how the input, gates, and cell interact within the model. As seen in the figure, the linear embedding layers are implemented before and after each VQC and act as feature encoders to transform the dimension of input features to the desired target dimension using matrix multiplication. In particular, when the target dimension is smaller than the input dimension, the output is a compressed feature representation. This type of embedding has been proven to significantly enhance quantum-enhanced RNN modeling [22].

In our QGRU-MC model, separate feature embeddings are prevalent for different VQCs. The separate linear embedding layer before VQCs maps the input data $[h_{t-1}, x_t]$ to a concatenated feature that is represented as $v_{t,i}$. By offering a distinct method for information mapping, the linear embedding layers that are implemented separately can facilitate an approach for non-linearity. After the computation in each VQC, the following separate linear embedding layer maps the output dimension to the hidden states dimension h_t. This can ensure distinct information mapping specially tailored to the corresponding

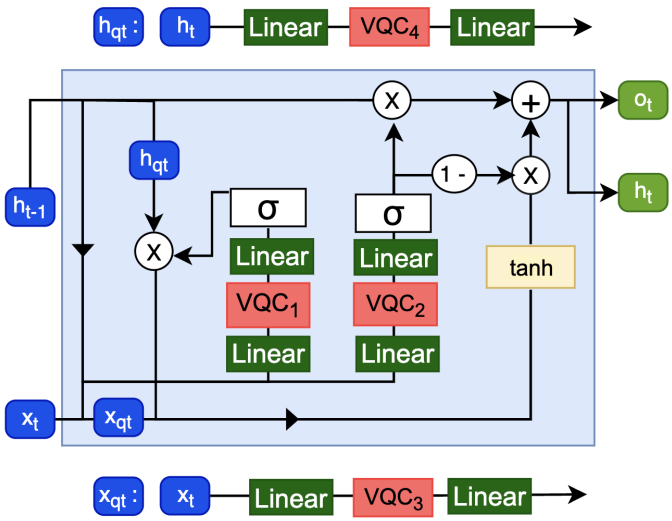

Fig. 3: QGRU embedding example including a linear enhanced embedding layer.

VQCs functionality. The formulae in the forward pass are expressed as follows:

$$y_{t,r} = L_{in,r}(v_t), \tag{1}$$
$$y_{t,u} = L_{in,u}(v_t), \tag{2}$$
$$x_q = L_{x,in}(x_t), \tag{3}$$
$$h_q = L_{h,in}(h_{t-1}), \tag{4}$$
$$r_t = \sigma(L_{r,out}(VQC_1(y_{t,r}))), \tag{5}$$
$$u_t = \sigma(L_{u,out}(VQC_2(y_{t,u}))), \tag{6}$$
$$\tilde{n_t} = L_{n1,out}(VQC_3(x_q)), \tag{7}$$
$$n_t = \tanh(\tilde{n_t} + u_t \odot L_{n2,out}(VQC_4(h_q))), \tag{8}$$
$$h_t = (1 - u_t) \odot n_t + u_t \odot h_{t-1}, \tag{9}$$

where v_t is the compressed output of $[h_{t-1}, x_t]$, $L_{in,r(u)}$ is the separate linear embedding layer for the reset and update gates, $L_{x(h),in}$ is a linear embedding layer for x and h_{t-1}, $L_{i,out}$ represents the linear layer after each VQC_i $(i = 1-4)$, and σ is the sigmoid activation function.

C. Multi-class Classifier

The output from QGRU is then passed through a three-layer feed-forward perceptron that classifies the data into corresponding activity-labeled categories called multi-class classifiers. In each layer, there is the implementation of batch normalization, and the last layer includes a rectified linear unit (ReLU) activation function to improve the training stability and model performance. Moreover, a drop-out layer is included in the third hidden layer to prevent overfitting. The output from this multi-class classifier will be used for post-processing with the softmax activation to output the probabilities for each class. This allows the QGRU-MC to predict the most likely correct class for a given input sequence. This hybrid architecture aims to utilize the temporal learning capabilities of QGRU, the advantage of quantum circuits with modern quantum-based hardware, and the spatial feature extraction strength of neural networks.

D. Optimization

QGRU-MC, like classical machine learning models, is trained for the data-driven task which involves the optimization of both classical and quantum parameters to minimize the prediction error. The classical parameters pertain to linear layers and post-quantum computation in the QGRU cell, while the quantum parameters are related to the rotation angles in the quantum circuits. This learning process employs the gradient-based optimization techniques including the mitigation of the loss function, $L(\theta)$, which is referred to as the objective function. These gradients are then used to iteratively update the parameters, aiming to accomplish convergence to an optimal set of values that potentially reduce the overall error, while increasing the model accuracy. This strategy involves iteratively adjusting parameters to get the highest substantial drop in the loss function, which is written as:

$$\theta_j \leftarrow \theta_j - \eta \nabla_{\theta_j} L(\theta), \tag{10}$$

where ∇_θ is the gradient and η is the learning rate.

The optimization process involves computing gradients using a type of forward-mode automatic differentiation that utilizes the parameter-shift rules for quantum parameters [14]. The gradient calculation of a VQC using the parameter-shift method can be expressed as:

$$\nabla_\theta f(x,\theta) = \frac{1}{2}[f(x,\theta+\frac{\pi}{2}) - f(x,\theta-\frac{\pi}{2})], \tag{11}$$

where $f(x,\theta)$ is the output function.

IV. Result and Discussion

For our results, we evaluate the model performance in terms of evaluation metrics and the confusion matrix. The model is trained in Python using the Pennylane library as a quantum simulator for quantum computation. The dataset is split into training (80%) and test (20%) sets. Moreover, we further split the training set into sub-train (80%) and validate (20%) sets.

A. Loss and Accuracy

Fig. 4 presents the training and validation loss and accuracy upon application of our QGRU-MC model to the ADL dataset. In both cases, there is a consistent decrease, indicating an effective learning and optimization process that minimizes the error during the training process. As seen in Fig. 4, the loss values stabilize after ~ 60 epochs, indicating we have reached convergence.

In terms of model accuracy, the accuracy trends for both training and validation datasets gradually increase during the training process with validation accuracy only slightly surpassing the training one towards the end. This pattern displays a good learning process of the model and also shows that the model generalizes well to unseen data without overfitting.

B. Confusion matrix and classification report

To provide a more comprehensive evaluation, we include the classification report and confusion matrix. Those tools not only provide detailed insights into model performance but also reveal the strengths and weaknesses in classifying each

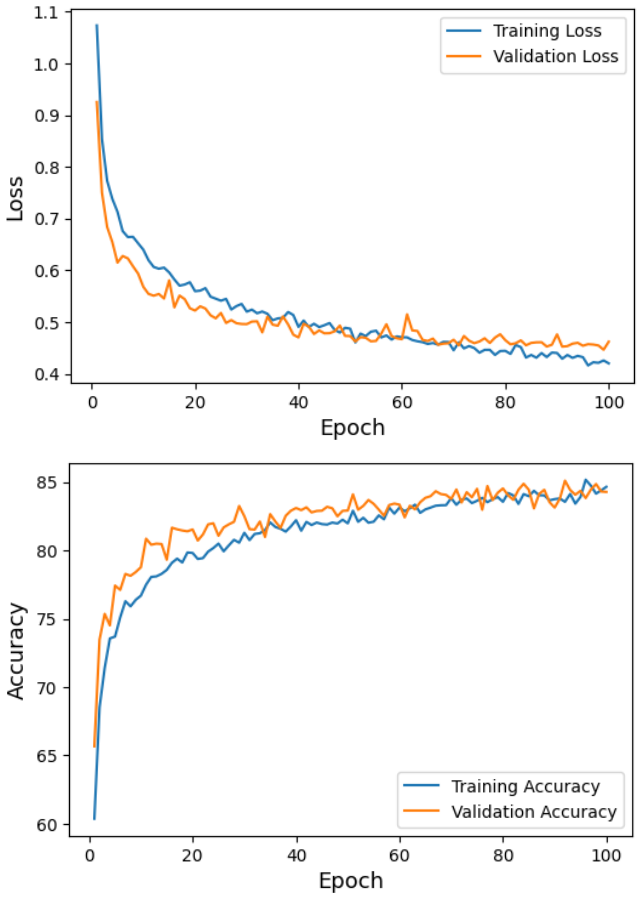

Fig. 4: QGRU-MC training and validation loss (top) and accuracy (bottom).

category. The confusion matrix presented in Fig. 5 shows the model performs extremely well in classifying classes 2 and 6, as indicated by a high number of correct predictions (244 and 56, respectively). In contrast, our model struggles with differentiating between classes 1 and 3 as there are 49 records of class 3 incorrectly predicted as class 1. Further, the model tends to misclassify 49 records of climbing or descending stairs (class 3) as walking (class 1). This misclassification can be based on the fact that both movements share similar patterns which is difficult to discern.

The classification report shown in Table II which summarizes the precision, recall, and F1 score for each class. The model achieves an overall accuracy of 79%, indicating a reasonably good ability to correctly classify instances across the eight different classes. Looking into detail for each class performance, the model displays its strongest performance when classifying records belonging to class 2, achieving a precision of 0.91 and a recall of 0.96, which result in an F1-score of 0.93. These high values suggest that the model accurately labels class 2 with minimal false positives. In contrast, the model faces challenges when identifying an instance of class 3, evidenced by a low recall score of 0.48 and an F1 score of 0.59.

Our model also performs well in classes 4 and 6. Classifying

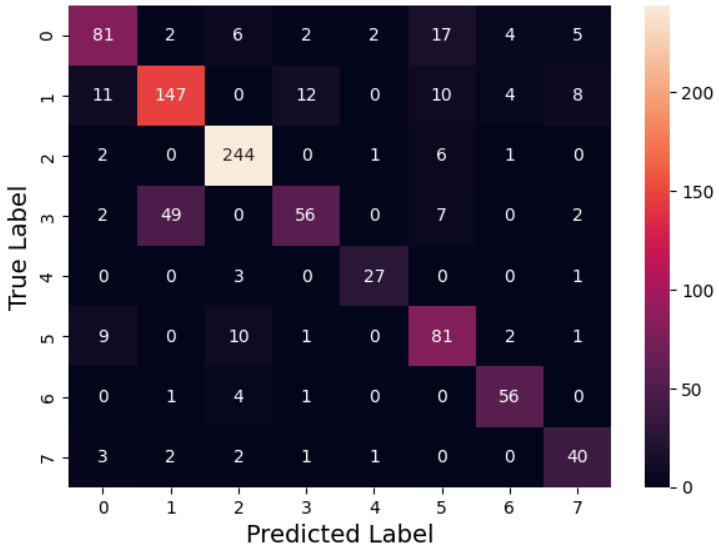

Fig. 5: Confusion matrix depicting performance of a multi-class classifier, illustrating the true versus predicted labels across the eight activity categories.

the class 4 model shows a strong performance with both precision and recall at 0.87, resulting in an F1-score of 0.72. In class 6, the model yielded a precision of 0.84 and a recall of 0.90, leading to an F1-score of 0.87. The confusion matrix shows 27 of 31 instances correctly classified for class 4 and 56 of 62 for class 6.

TABLE II: Classification report of the QGRU-MC model.

Class	Support	Precision	Recall	F1-score
0	119	0.75	0.68	0.71
1	192	0.73	0.77	0.75
2	254	0.91	0.96	0.93
3	116	0.77	0.48	0.59
4	31	0.87	0.87	0.87
5	104	0.67	0.78	0.72
6	62	0.84	0.90	0.87
7	49	0.70	0.82	0.75
	Accuracy		0.79	
	Macro avg	0.78	0.78	0.78
	Weighted avg	0.79	0.79	0.78

On the other hand, moderate performance is noted in classifying classes 1, 5, and 7. For classes 1 and 5, the model achieves precision of 0.73 and 0.67, recall of 0.77 and 0.78, and an F1-score of 0.75 and 0.72, respectively. For class 7, the model attains a precision of 0.70 and a higher recall of 0.82, compared to classes 1 and 5, and an F1-score of 0.75. Conversely, the model performs poorly in distinguishing class 0, with a precision of 0.75, a recall of 0.68, and F1-score of 0.71.

V. Conclusion

Our proposed model referred to as QGRU-MC was utilized to classify 14 daily activities through tri-axial accelerometer data collected from a wrist-worn device. Preliminary testing achieved an overall accuracy of 79% and a resulting F1-score of 0.78. Although this work shows promising performance in classifying ADLs to support healthy aging, further research and experimentation are necessary. The future plan includes further work on refining feature engineering, implementing advanced training techniques, and utilizing different datasets that support ADLs research. These efforts aim to reduce the number of misclassifications and improve the models overall evaluation metrics, especially for the classes with lower performance. From our results, the proposed QGRU-MC has great potential in learning and classifying complex data commonly encountered in healthcare.

Acknowledgement

This work was supported in part by the Canada Excellence Research Chair (CERC) Program CERC-2022-00109 and in part by the Canada Research Chair Program CRC-2022-00187.

References

[1] B. Barbara, Mastrogiovanni, Fulvio, S. Antonio, V. Tullio, and Z. Renato, "Analysis of human behavior recognition algorithms based on acceleration data," in *2013 IEEE International Conference on Robotics and Automation*, Karlsruhe, Germany, May 2013.

[2] L. Nygård, "Instrumental activities of daily living: a stepping-stone towards alzheimer's disease diagnosis in subjects with mild cognitive impairment?" *Acta neurologica Scandinavica. Supplementum*, vol. 179, pp. 42–6, Feb. 2003.

[3] R. S. Bucks, D. L. Ashworth, G. K. Wilcock, and K. Siegfried, "Assessment of activities of daily living in dementia: Development of the bristol activities of daily living scale," *Age and Ageing*, vol. 25, no. 2, Mar. 1996.

[4] C. Debes, A. Merentitis, S. Sukhanov, M. Niessen, N. Frangiadakis, and A. Bauer, "Monitoring activities of daily living in smart homes: Understanding human behavior," *IEEE Signal Processing Magazine*, vol. 33, no. 2, pp. 81–94, Mar. 2016.

[5] M. Haghi, K. Thurow, and R. Stoll, "Wearable devices in medical internet of things: Scientific research and commercially available devices," *Healthcare informatics research*, vol. 23, no. 1, Jan. 2017.

[6] L. Atallah, B. Lo, R. Ali, R. King, and Y. Guang-Zhong, "Real-time activity classification using ambient and wearable sensors," *IEEE Trans. Inform. Technol. Biomed.*, vol. 13, no. 6, Nov. 2009.

[7] B. Ling and I. S. S., "Activity recognition from user-annotated acceleration data," in *Pervasive*, vol. 3001. Berlin, Germany: Springer, Apr. 2004, pp. 1–17.

[8] S. Li and J. Xu, "A recurrent neural network language model based on word embedding," Macau, China, Jul. 2018.

[9] K. Lee, C. Park, N. Kim, and J. Lee, "Accelerating recurrent neural network language model based online speech recognition system," in *2018 IEEE International Conference on Acoustics, Speech and Signal Processing (ICASSP)*, Calgary, Canada, Apr. 2018, pp. 5904–5908.

[10] R. Jurca, T. Cioara, I. Anghel, M. Antal, C. Antal, and D. Moldovan, "Activities of daily living classification using recurrent neural networks," in *2018 17th RoEduNet Conference: Networking in Education and Research (RoEduNet)*, Cluj-Napoca, Romania, Sep. 2018, pp. 1–4.

[11] S. Aishwarya, V. Abeer, B. B. Sathish, and K. N. Subramanya, "Quantum computational techniques for prediction of cognitive state of human mind from eeg signals," *Journal of Quantum Computing*, vol. 2, no. 4, pp. 157–170, Jan. 2021.

[12] V. Gandhi, G. Prasad, D. Coyle, L. Behera, and T. M. McGinnity, "Quantum neural network-based eeg filtering for a brain-computer interface," *IEEE Transactions on Neural Networks and Learning Systems*, vol. 25, no. 2, pp. 278–288, Feb. 2014.

[13] B.-N. D. Tran, M. Fahim, A. A. Cheema, S. Czarnuch, B. D. E. McNiven, O. A. Dobre, and T. Q. Duong, "Estimation of energy expenditure in wearable healthcare technology by quantum-based lstm modeling," in *IEEE International Conference on Quantum Communications, Networking, and Computing (QCNC 2024)*, Kanazawa,Japan, Jul. 2024.

[14] K. Mitarai, M. Negoro, M. Kitagawa, and K. Fujii, "Quantum circuit learning," *Phys. Rev. A*, vol. 98, p. 032309, Sep 2018.

[15] M. Benedetti, E. Lloyd, S. Sack, and M. Fiorentini, "Parameterized quantum circuits as machine learning models," *Quantum Science and Technology*, vol. 4, no. 4, p. 043001, Nov. 2019.

[16] D. Yuxuan, H. Min-Hsiu, T. Liu, and D. Tao, "Expressive power of parametrized quantum circuits," *Phys. Rev. Res.*, vol. 2, p. 033125, Jul. 2020.

[17] L. T, P. A. J., and S. A. Yu, "Entanglement in a quantum annealing processor," *Phys. Rev. X*, vol. 4, p. 021041, May 2014.

[18] M. F. Bruno, Barbara and A. Sgorbissa, "Dataset for adl recognition with wrist-worn accelerometer," UCI Machine Learning Repository, Feb. 2014.

[19] N. Chawla, K. Bowyer, L. Hall, and W. Kegelmeyer, "Smote: Synthetic minority over-sampling technique," *Journal of Artificial Intelligence Research*, vol. 16, pp. 321–357, Jun. 2002.

[20] D. Wilson, "Asymptotic properties of nearest neighbor rules using edited data," *IEEE Transactions on Systems, Man, and Cybernetics*, vol. SMC-2, no. 3, pp. 408–421, Jul. 1972.

[21] S. J. Preece, J. Y. Goulermas, L. P. Kenney, and D. Howard, "A comparison of feature extraction methods for the classification of dynamic activities from accelerometer data," *IEEE Transactions on Biomedical Engineering*, vol. 56, no. 3, pp. 871–879, Apr. 2008.

[22] C. Yuji, Z. Xiyuan, F. Xiang, Z. Huan, L. Wenxuan, and ZhaoJunhua, "Linear-layer-enhanced quantum long short-term memory for carbon price forecasting," *Quantum Machine Intelligence*, vol. 5, Jul. 2023.

[23] S. Sukin, J. P. D., and A.-G. Alán, "Expressibility and entangling capability of parameterized quantum circuits for hybrid quantum-classical algorithms," *Advanced Quantum Technologies*, vol. 2, no. 12, p. 1900070, May 2019.